Supporting Information

Competitive Binding Assay with an Umbelliferone-based Fluorescent Rexinoid for Retinoid X Receptor Ligand Screening

Shoya Yamada,[†,‡] Mayu Kawasaki,[⊥] Michiko Fujihara,[†,§] Masaki Watanabe,[†] Yuta Takamura,[†] Maho Takioku,[†] Hiromi Nishioka,[†] Makoto Makishima,[‖] Yasuo Takeuchi,[†] Tomoharu Motoyama,[⊥] Sohei Ito,[⊥] Hiroaki Tokiwa,[#,¶] Shogo Nakano,[*,⊥] and Hiroki Kakuta[*,†]

[†]Division of Pharmaceutical Sciences, Okayama University Graduate School of Medicine, Dentistry and Pharmaceutical Sciences, 1-1-1, Tsushima-naka, Kita-ku Okayama 700-8530, Japan.
[‡]Research Fellowship Division, Japan Society for the Promotion of Science, Sumitomo-Ichibancho FS Bldg., 8 Ichibancho, Chiyoda-ku, Tokyo102-8472, Japan.
[§]AIBIOS Co. Ltd. Tri-Seven Roppongi 8F 7-7-7 Roppongi, Minato-ku, Tokyo 106-0032 Japan.
[‖]Division of Biochemistry, Department of Biomedical Sciences, Nihon University School of Medicine, 30-1 Oyaguchi-kamicho, Itabashi-ku, Tokyo 173-8610, Japan.
[⊥]Graduate School of Integrated Pharmaceutical and Nutritional Sciences, University of Shizuoka, 52-1 Yada, Suruga-ku, Shizuoka 422-8526, Japan.
[#]Department of Chemistry and [¶]Research Center of Smart Molecules, Rikkyo University, Nishi-ikebukuro, Toshimaku, Tokyo 171-8501, Japan.

E-mail: snakano@u-shizuoka-ken.ac.jp (S.N.)
kakuta-h@okayama-u.ac.jp (H.K.)

Contents:

1. In vitro assays

Crystallization and X-ray data collection of RXRα-LBD/10

For crystallization of the extended state of RXRα-LBD complexed with **10** (RXRα-LBD/**10**), the receptor was firstly dialyzed against buffer containing 20 mM HEPES-NaOH (pH 8.0), 100 mM NaCl and 5% (v/v) glycerol, then concentrated utilizing an Amicon Ultra-15 centrifugal filter (Millipore). The receptor and **10** were mixed in a molar ratio of 1 (protein): 3 (**10**), and incubated for 12 hrs at 4 ºC. Crystals of RXRα-LBD/**10** appeared under the conditions of PEG-ION Screen 1-25 [20% (w/v) polyethylene glycol 3350 and 0.2 M $Mg(OAc)_2$] at 22 ºC.

The obtained crystals were soaked in 20% (v/v) glycerol, mounted, and flash-cooled under a nitrogen stream at -173 ºC. Diffraction data were collected using an ADSC Quantum 270 at NW12A and PILATUS3 S 2M at BL5A at the Photon Factory (Tsukuba, Japan). The data were collected, scaled and integrated by HKL2000 and SCALEPACK (reference S1). The initial phase was determined by the molecular replacement method with MOLREP(reference S2) utilizing the structure of 5GYM for RXRα-LBD/**3** as a template. Model building and structure refinement were performed by COOT (reference S3) and REFMAC (reference S4), respectively. All figures were prepared by PyMOL (reference S5). Crystallographic parameters are shown in Table S1.

UV–vis and fluorescence spectra measurements

Absorbance spectra were recorded on a Jasco v-530. Fluorescence spectra were recorded on Hitachi F-4500 using a quartz cuvette (5 mm). Analytical grade solvents were obtained from Wako and used as received. The excitation wavelength of fluorescence spectra of **10** was set at 355 nm for MeOH solution, and at 396 nm for 0.1 N NaOH solution, and emission was detected from 600 nm to 370 nm. The excitation and emission slit widths of **10** were 10 nm and 10 nm, respectively. Relative fluorescence intensity of 100 nM **10** in various solvents containing 1% DMSO was determined at Ex/Em = 360 nm/465 nm.

Fluorescence quantum yield determination

Fluorescence quantum yield of **10** was determined according to reference S6. (-)-Quinine sulfate in 0.1 M H_2SO_4 was used as a standard ($\Phi F = 0.55$) (reference S7). The excitation wavelength was set at 355 nm, and emission was detected from 600 nm to 370 nm. The fluorescence quantum yield of **10** was 0.47 ± 0.00 in 0.1 N NaOH and 0.09 ± 0.02 in MeOH.

Preparation of human RXRα-LBD

A plasmid containing human RXRα-LBD (residues 224-462) cloned into pET28a vector was transformed into *E. coli* BL21(DE3) strain. Overexpression was performed by following the same protocol as in the previous study (reference S8). Cells were collected and resuspended into buffer A containing 20 mM HEPES-NaOH (pH 8.0), 100 mM NaCl, 0.5 mM TCEP and 5% (v/v) glycerol. After sonication, insoluble material was removed by centrifugation at 10000×*g* for 30 min. The obtained supernatant was applied to a HisTrap HP column (GE Healthcare). The column was washed with buffer A containing 70 mM imidazole, and eluted with buffer A containing 300 mM imidazole. The His-tag was cleaved by reacting the samples with 200 U of thrombin at 4 ºC for 2 days. The cleaved samples were concentrated and applied to a gel filtration column (Superdex 200 pg Increase) equilibrated with buffer A. Fractions containing samples were collected, and used for experiments after confirmation of their purity by SDS-PAGE.

***K*d determination of CU-6PMN (10)**

Assay conditions were as described in reference S9. Assay buffer for this assay contained 10 mM Hepes, 150 mM NaCl, 2 mM $MgCl_2$, 5 mM DTT at pH 7.9. Final DMSO concentration was 1% (not considering DMSO used to dissolve fluorescein-peptides). Black 384-well microplates were purchased from Greiner Bio-One International (#784076). hRXRα-LBD, **3**, and **10** were diluted as required with the assay buffer described above.

This assay was performed according to SI Chart 1. To 4 wells per sample in a black 384-well plate were added 10 µL of two-fold serial dilutions of hRXRα-LBD (final concentrations of 4,000–31 nM) in 1% DMSO assay buffer, 5 µL of 1,200 nM of **10** (300 nM final concentration) and 5 µL of 1% DMSO assay buffer or 40 µM bexarotene (10 µM final concentration) in 1% DMSO assay buffer. The plate was kept in the dark at r.t. for 2 hours. Data were collected at Ex/Em=360 nm/465 nm using a Tecan Infinite F200. Data exclusion was performed using the Q-test (reference S10). The specific equilibrium binding constant (*K*d) was derived from the specific binding curve by fitting the data to a sigmoid equation using Excel software.

Transformation of measured fluorescence intensity into bound receptor concentration

The measured fluorescent intensity (Fl_{obs}) was transformed into bound receptor concentration (Rb) using equation S1, modified from reference S11,

$$Rb = Lt \times [(Fl_{obs} - Fl_{min}) / (Fl_{max} - Fl_{min})] \text{ -------- (S1)}$$

where Lt, Fl_{max}, and Fl_{min} are the total ligand concentration, and the fluorescence intensities when the fluorescent ligand was completely bound and not bound to hRXRα-LBD, respectively. The free receptor concentration (Rf) was calculated by subtracting Rb from the total receptor concentration. The bound ligand concentration (B) was assumed to be equal to Rb, and the free ligand concentration (F) was calculated by subtracting B from Lt. On the basis of the above calculations, Scatchard and Hill plots were prepared.

Binding assay of a panel of RXR ligands with hRXRα-LBD using CU-6PMN (10)

This assay was performed according to SI Chart 2 using similar materials to those used for *K*d determination of **10**. Two-fold serial dilutions of each test compound (100 μM to 0.2 μM, 10 concentration levels) were incubated with 100 nM **10**, 500 nM hRXRα-LBD as final concentrations in the assay buffer described above at r.t. for 2 hours. Final DMSO concentration was 1%. Data were collected at Ex/Em=360 nm/465 nm. IC_{50} was derived from the binding curve by fitting the data into a sigmoid equation using Excel software. The inhibition constant (*K*i) value was calculated by using equation 1. The *K*i values were used to compare the binding affinities of test compounds to hRXRα-LBD.

To 4 wells each in a black 384-well plate were added 10 μL of 1,000 nM hRXRα-LBD in 1% DMSO assay buffer, 5 μL of two-fold serial dilutions of test compound in 1% DMSO assay buffer (final concentrations of 16 μ–31 nM), and 5 μL of 400 nM of **10** (100 nM final concentration). The plate was kept in the dark at r.t. for 2 hours. Data were collected at Ex/Em=360 nm/465 nm using a Tecan Infinite F200. Data exclusion was performed using the Q-test (reference S10). The specific equilibrium binding constant (*K*d) was derived from the specific binding curve by fitting the data to a sigmoid equation using Excel software.

Z'-factor

In the Z'-factor signal stability test, 8 data points were included in each high-signal (10 μM **3**, positive control to determine nonspecific binding) or low-signal (DMSO, negative vehicle control to determine total binding) group, and the Z'-factor value was calculated by using equation S2 (reference S12),

$$Z' = 1 - [(3\sigma+ + 3\sigma-)/(M+ - M-)] \text{ -------- (S2)}$$

where σ+ is the standard deviation of the positive control (10 μM **3**) group, σ- is the standard deviation of the negative control (DMSO) group, M+ is the mean of the positive control (10 μM **3**) group, and M- is the mean of the negative control (DMSO) group.

Statistical analysis

Results are expressed as the mean ± standard deviation of at least three independent experiments.

2. Figure S1.

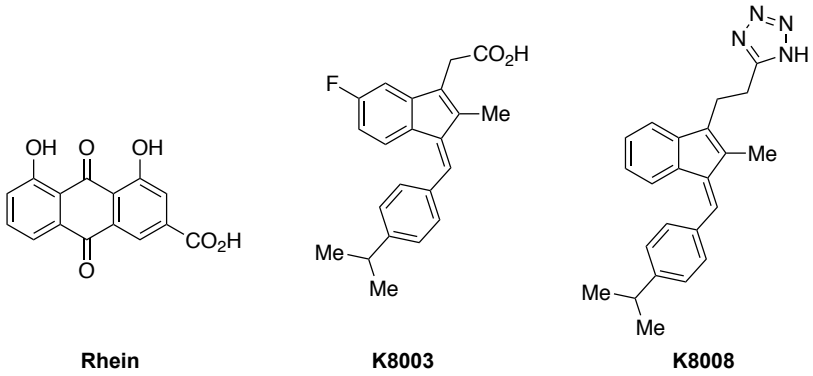

Figure S1. Chemical structures of the compounds used in Figure 3.

3. Figure S2.

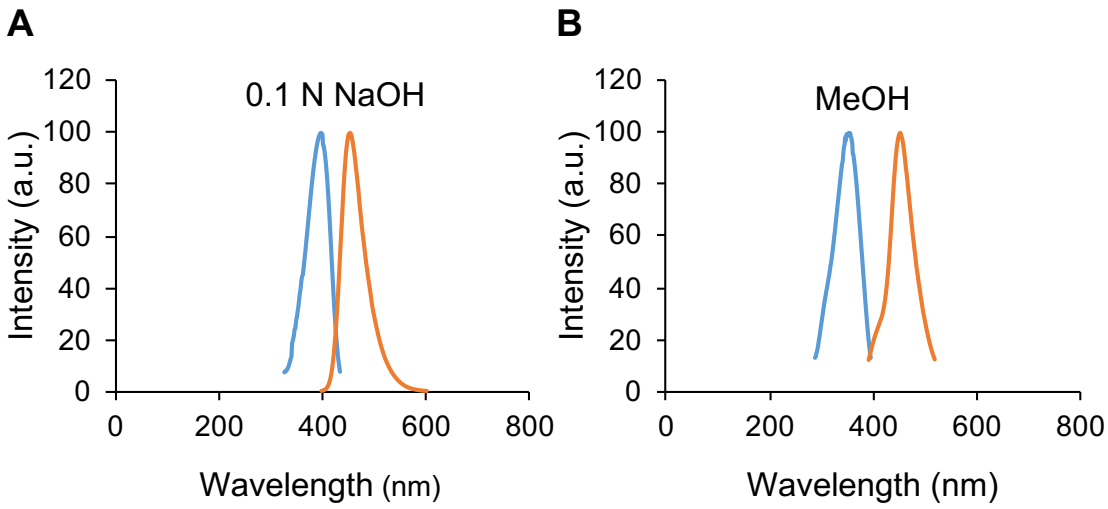

Figure S2. Relative absorbance and fluorescence spectra of **10** in 0.1 N NaOH (A) and MeOH (B). The spectra were obtained at Ex 396 nm in 0.1 N NaOH and Ex 352 nm in MeOH.

4. Figure S3.

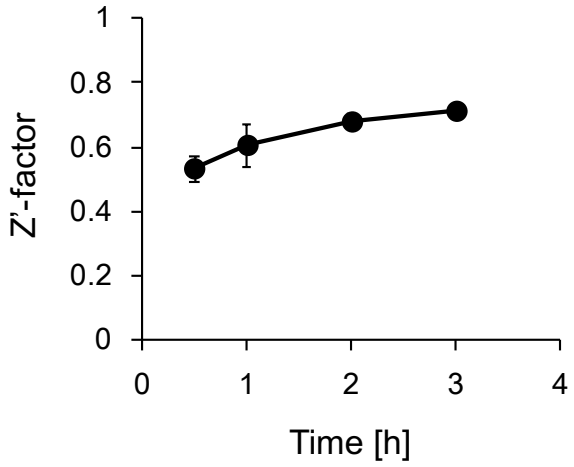

Figure S3. Time comparison of Z'-factors obtained using 100 nM **10** and 10 μM **3** with 0.5 μM hRXRα-LBD. n = 3, mean ± SD.

5. Figure S4.

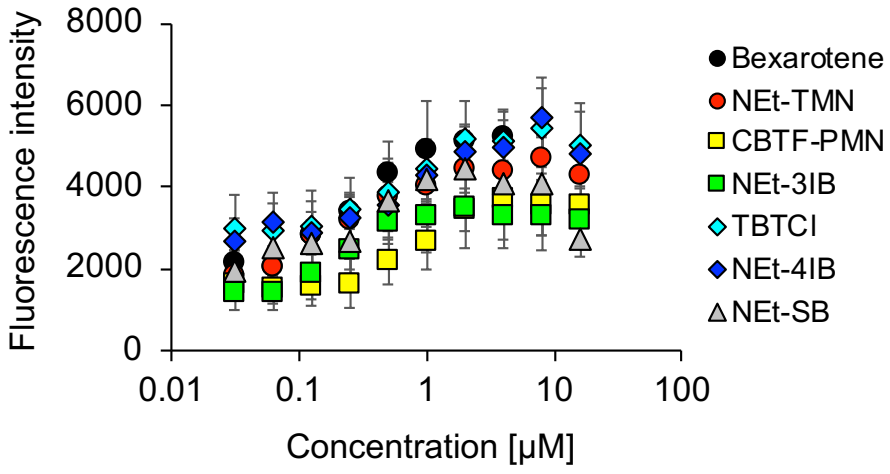

Figure S4. Fluorescence intensity curves of the test compounds in the assay using **10**. Fluorescence intensity was obtained by subtraction of the fluorescence of hRXRα-LBD with the test compound in the absence of **10** from that in the presence of **10**. This assay was performed using a 384-well plate

(4 wells/sample). Final concentrations of **10** and hRXRα-LBD were 0.1 μM and 0.5 μM, respectively. Each compound was added at 0.03125, 0.0625, 0.125, 0.25, 0.5, 1, 2, 4, 8 and 16 μM (final concentrations). The assay buffer contained 10 mM Hepes, 150 mM NaCl, 2 mM $MgCl_2$, 5 mM DTT (pH 7.9). DMSO final concentration was 1%. Fluorescence was measured at Ex 360 nm/Em 465 nm. Data shown are mean ± SD (n = 4). The *K*i value was obtained from the calculated sigmoidal curve and shown in Table S3. Chemical structures of the compounds used are shown in Figure S4.

6. Figure S5.

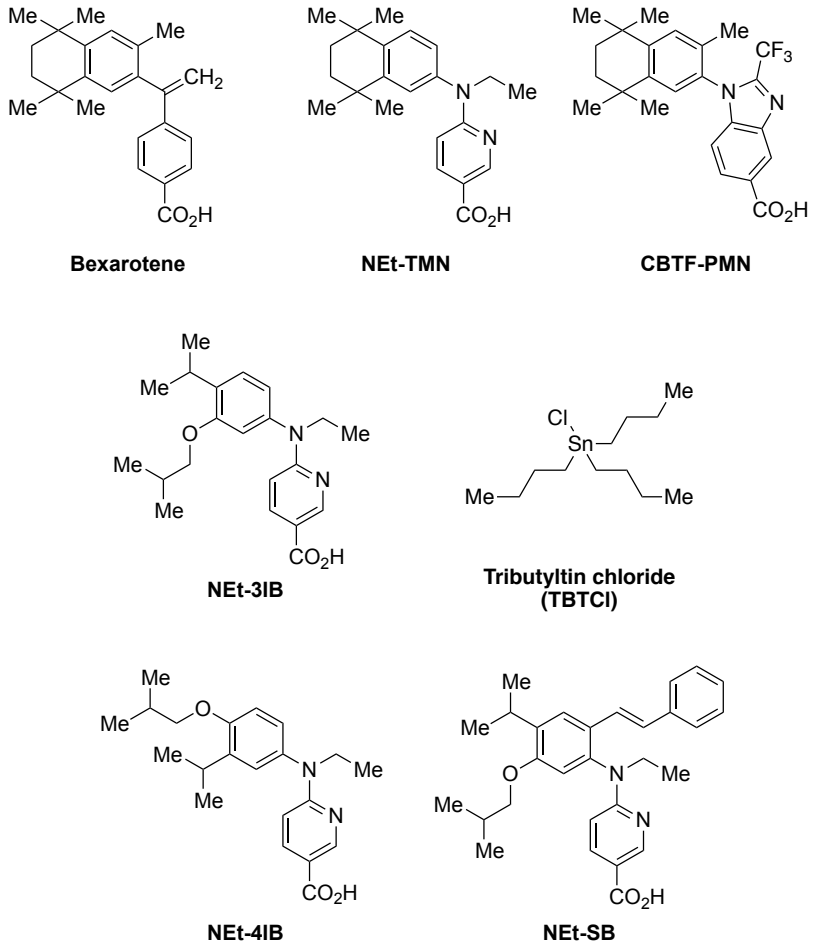

Figure S5. Chemical structures of the compounds used in Figure S4.

7. Figure S6.

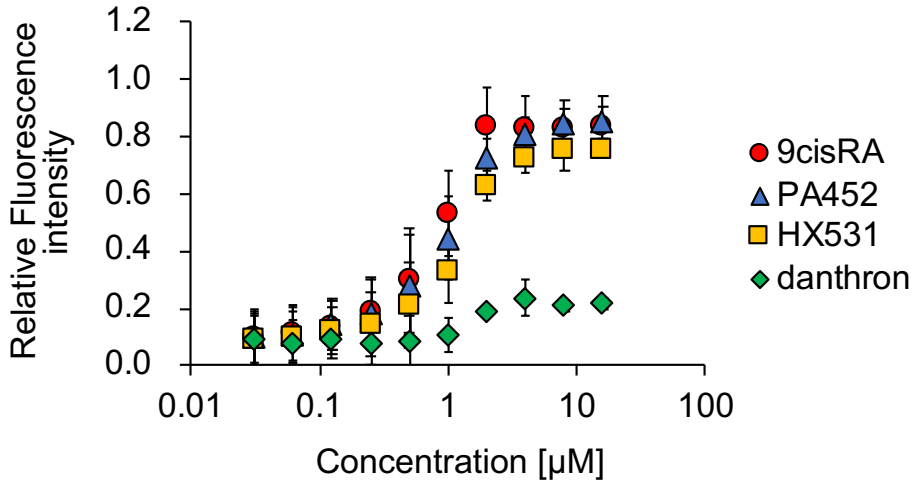

Figure S6. Relative fluorescence intensity curves of 9*cis*-retinoic acid (**1**), and RXR antagonists in the assay using **10**. The y-axis is shown as the relative value to 10 μM **3**, taken as 1 (positive control). Data shown are mean ± SD (n = 3). The *K*i value was obtained from the calculated sigmoidal curve and shown in Table S3. For danthron, the compound precipitation over 8 μM is suspected. Chemical structures of the compounds used except **1** are shown in Figure S7.

8. Figure S7.

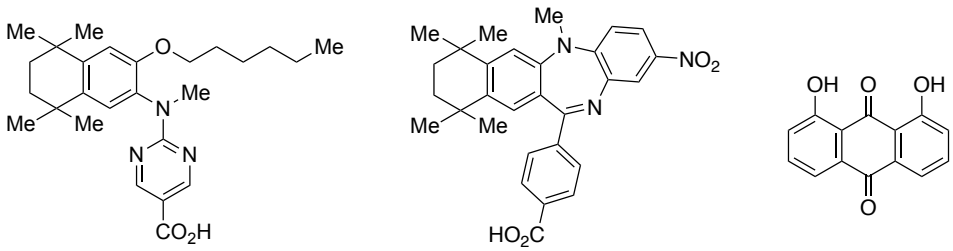

Figure S7. Chemical structures of RXR antagonists used in Figure S4. PA452, HX531, and danthron were referred to references 13, 14, and 15, respectively.

9. Chart S1. Protocol for Saturation Assay of 10 toward hRXRα-LBD.

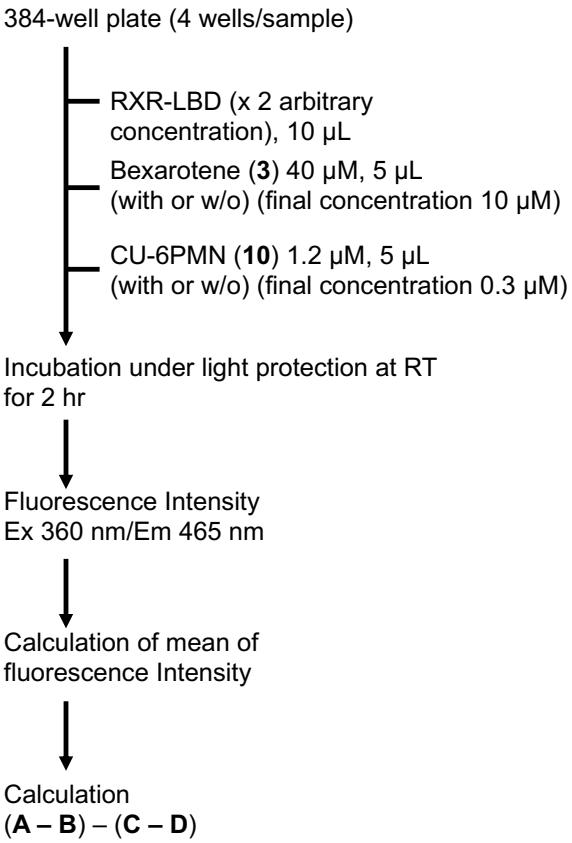

	CU-6PMN (**10**)	Bexarotene (**3**)	hRXRα-LBD
A	+	-	+
B	-	-	+
C	+	+	+
D	-	+	+

10. Chart S2. Assay Protocol for Test compounds.

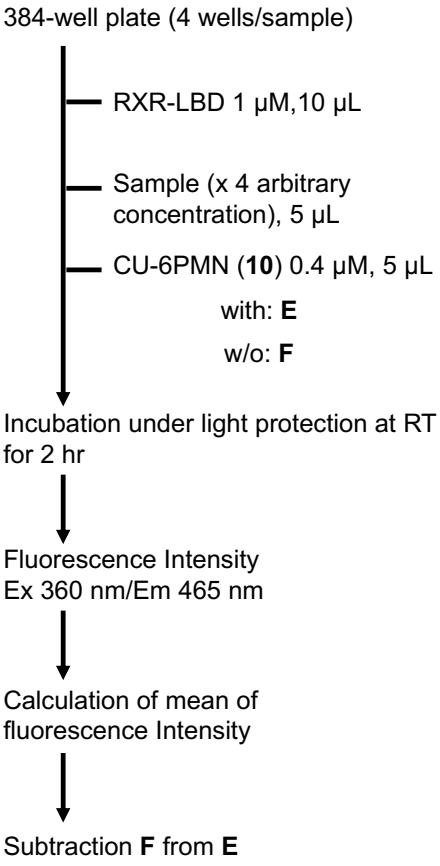

	CU-6PMN (**10**)	sample	hRXRα-LBD
E	+	+	+
F	-	+	+

11. Table S1.

Table S1. X-Ray diffraction statistics for hRXRα-LBD (224-462) complexed with **10**

Space group	$P2_1$
Unit cell parameters	
a (Å)	46.62
b (Å)	99.39
c (Å)	110.2
α (degree)	90.0
β (degree)	99.4
γ (degree)	90.0
X-ray source	PF-AR NW12A
Wavelength (Å)	1.00
Resolution (Å)	46.0–2.65 (2.72–2.65)
No. of reflections[a]	193032
No. of unique reflections	27286
Completeness (%)	99.7 (95.8)
I/sig(I)	10.7 (1.3)
R_{merge}[b]	0.134 (0.716)
CC1/2	0.993 (0.706)
B of Wilson plot (Å)^2	37.9
R[c]	0.226
R_{free}[d]	0.274
RMSD of geometry	
Bond length (Å)	0.003
Bond angle (degree)	1.132
Geometry	
Ramachandran outlier (%)	0.1
Ramachandran favored (%)	99.9
Average *B* factor (Å)^2	
Protein atoms	54.0
Ligand atoms	61.4
Solvent atoms	44.8
PDB code	6JNO

[a] Sigma cutoff was set to none (F > 0σF).
[b] $R_{merge} = \Sigma_h\Sigma_i|I_i(h)-\langle I(h)\rangle|/\Sigma_h I(h)$, where $I_i(h)$ is the i^{th} measurement of reflection h, and $\langle I(h)\rangle$ is the mean value of the symmetry-related reflection intensities. Values in brackets are for the shell of the highest resolution.
[c] $R = \Sigma||F_o|-|F_c||/\Sigma|F_o|$, where F_o and F_c are the observed and calculated structure factors used in the refinement, respectively.
[d] R_{free} is the *R*-factor calculated using 5% of the reflections chosen at random and omitted from the refinement.
[e] n.d. means "not determined".

12. Table S2.

Table S2. Comparison of hRXRα-LBD binding affinity values obtained using **10** and [^{3}H]**1**

	*K*i (nM)	
	Fl (using **10**)	RI (using [^{3}H]**1**)
Bexarotene (3)	379 ± 79	201
NEt-TMN	212 ± 34	22
CBTF-PMN	733 ± 59	413
NEt-3IB	182 ± 18	9
NEt-4IB	567 ± 115	581
NEt-SB	336 ± 143	39
TBTCl	604 ± 128	649

The *K*i values using **10** and the *K*i values using [^{3}H]**1** toward hRXRα-LBD were obtained from the calculated sigmoidal curve shown in Figure S3.

13. Table S3.

Table S3. *K*i values of 9*cis*-retinoic acid (**1**), bexarotene (**3**), DHA, EPA, PA452, HX531, and danthron using **10**

	*K*i (nM)
	Fl (**10**, CU-6PMN)
9*cis*-Retinoic acid (1)	583 ± 158
Bexarotene (3)	379 ± 79
DHA	6292 ± 658
EPA	7632 ± 1797
PA452	730 ± 170
HX531	906 ± 68
danthron	N.D.

The *K*i values were obtained from the calculated sigmoidal curve shown in Figure 5B and Figure S6. n = 3, mean ± SD. N.D. means “not determinable”.

14. NMR Charts

10: ^{1}H NMR chart (DMSO-*d*6)

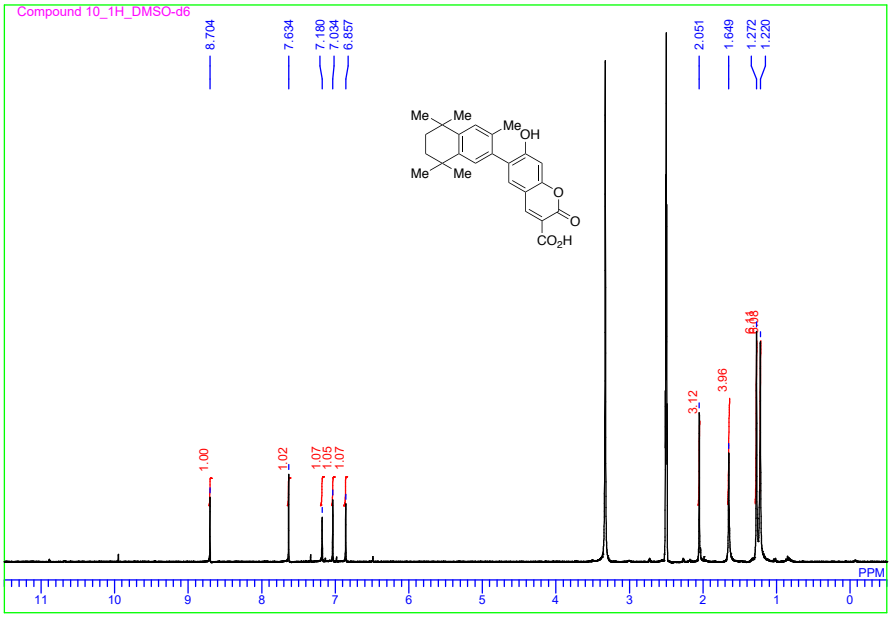

10: ^{13}C NMR chart ($CDCl_3$)

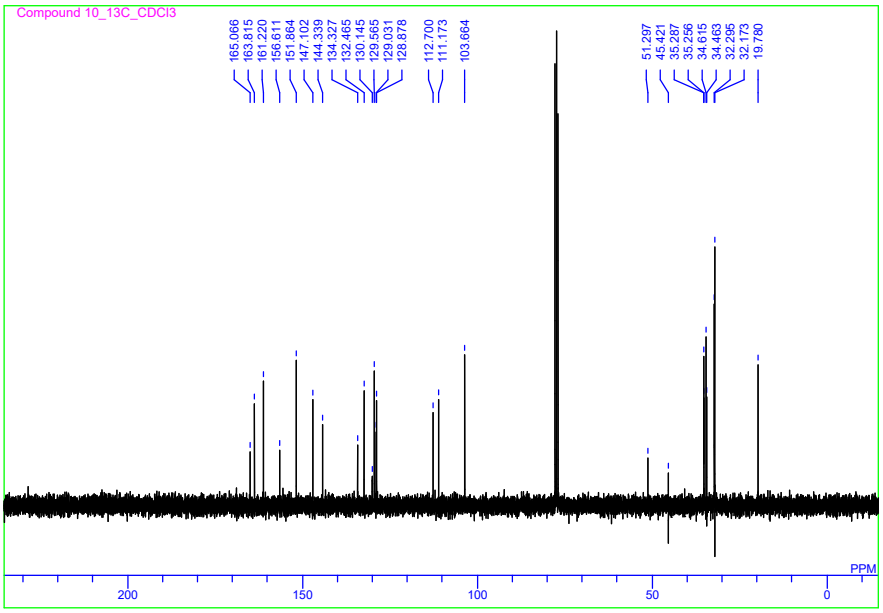

11: ^{1}H NMR chart ($CDCl_3$)

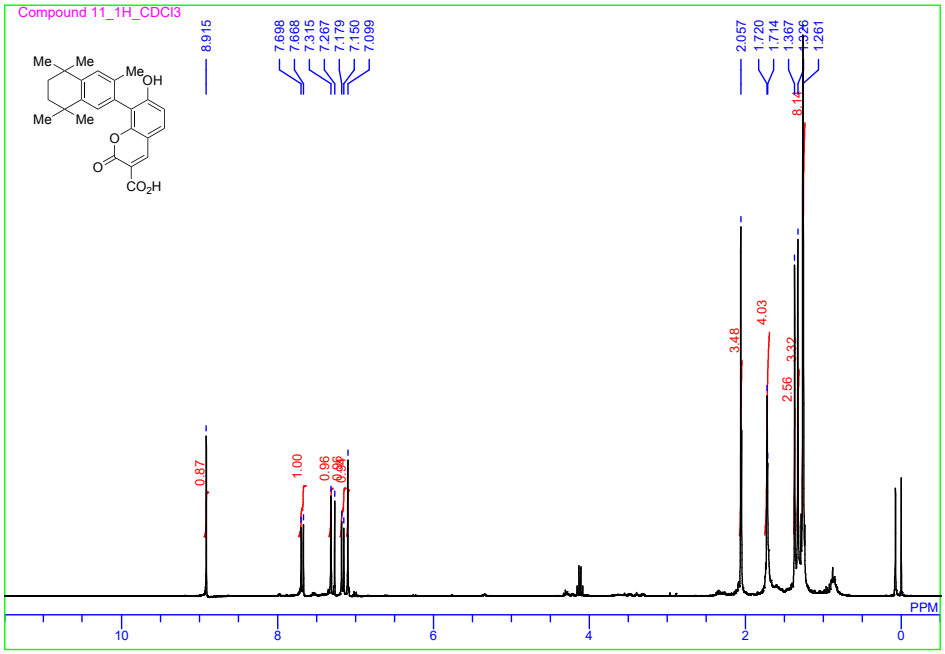

11: ^{13}C NMR chart ($CDCl_3$)

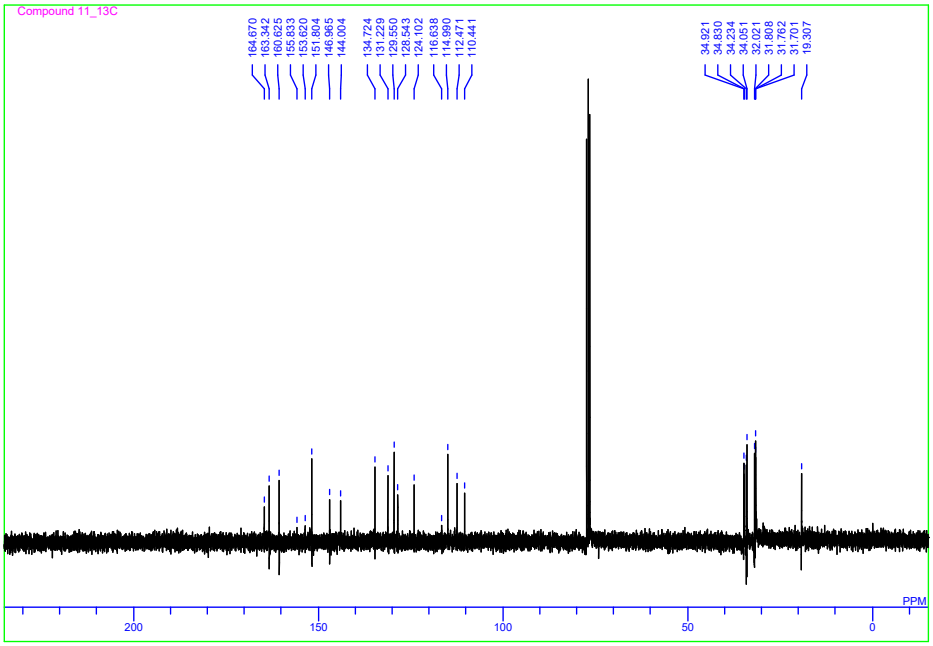

14: ^{1}H NMR chart ($CDCl_3$)

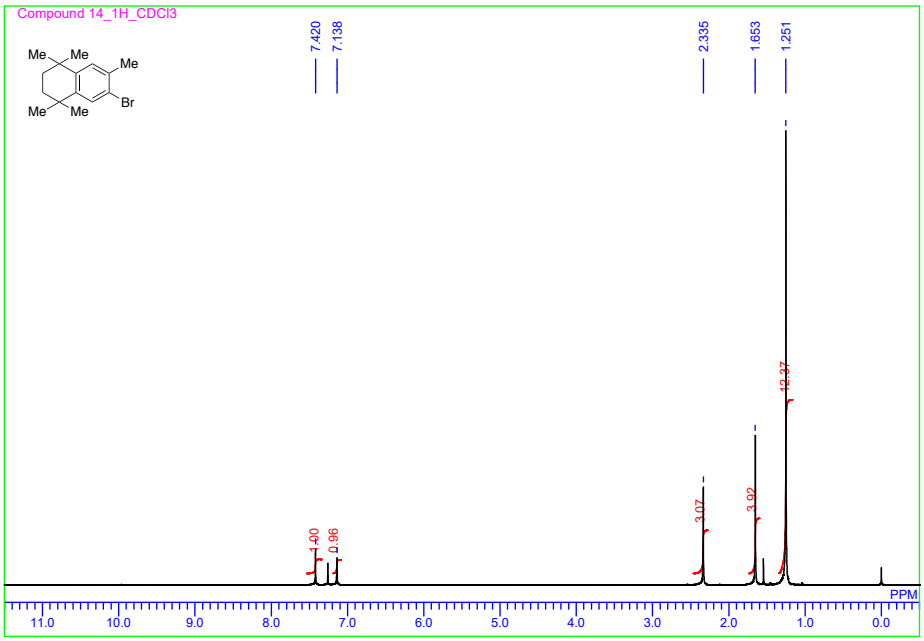

14: ^{13}C NMR chart ($CDCl_3$)

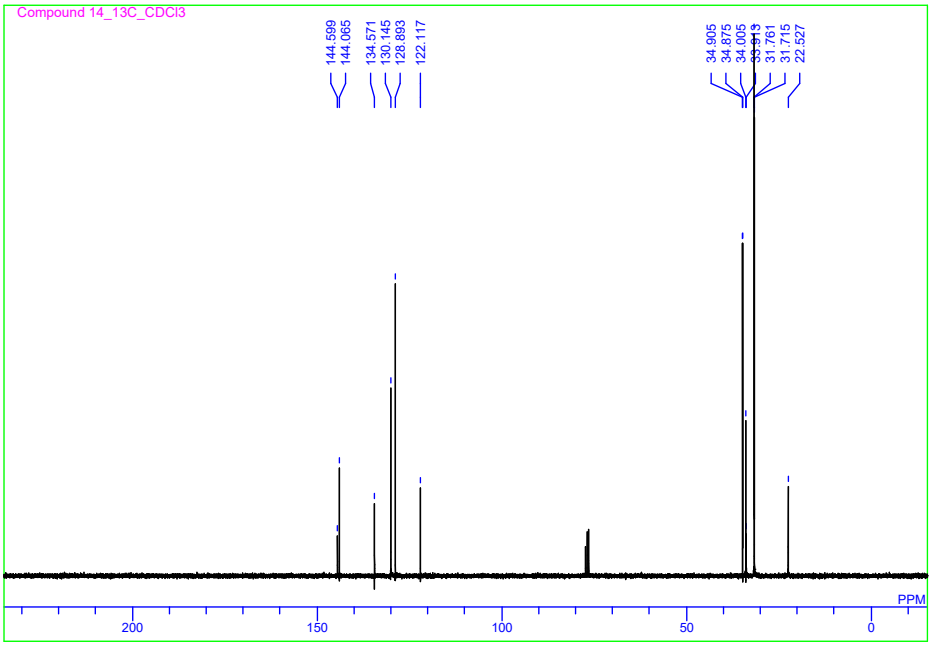

15: ^{1}H NMR chart ($CDCl_3$)

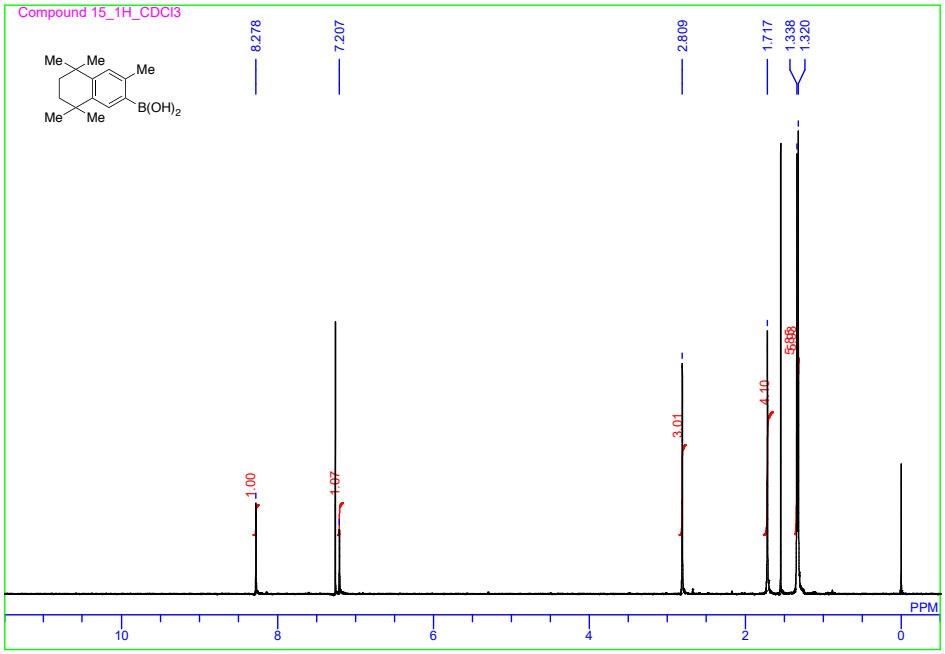

15: ^{13}C NMR chart ($CDCl_3$)

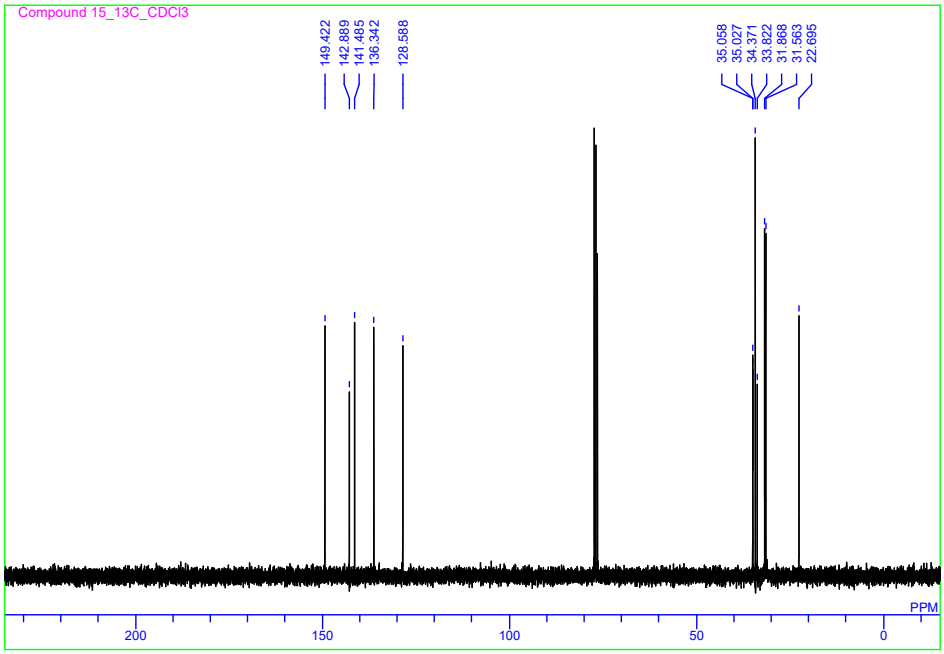

17: ^{1}H NMR chart ($CDCl_3$)

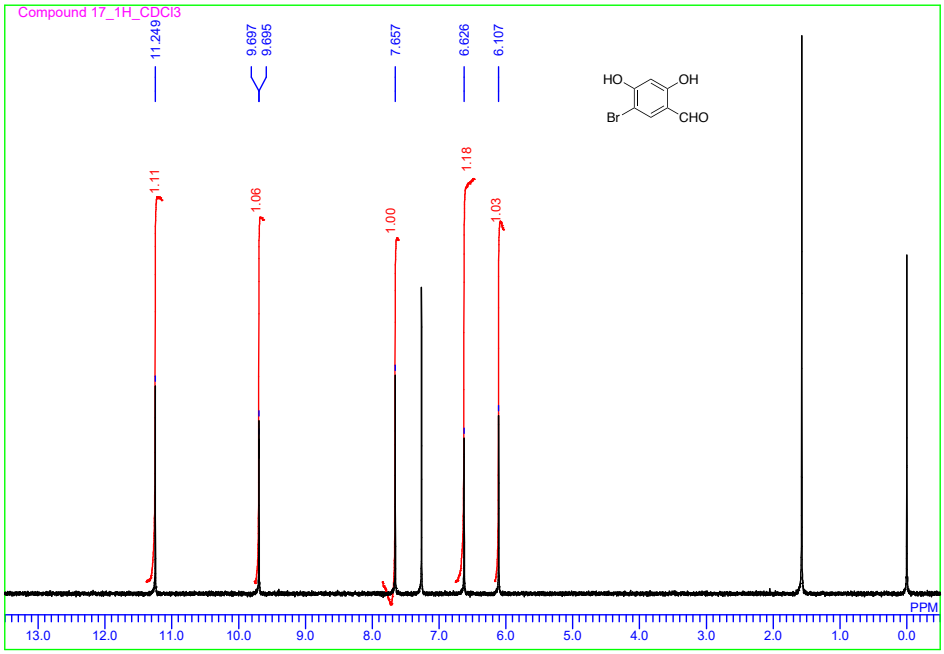

18: ^{1}H NMR chart ($CDCl_3$)

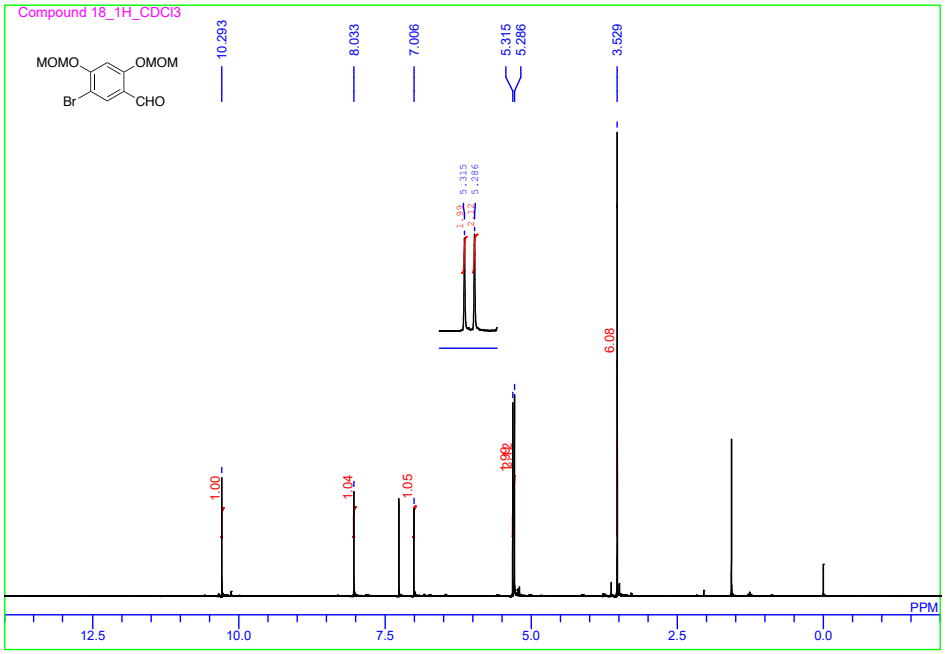

18: ^{13}C NMR chart ($CDCl_3$)

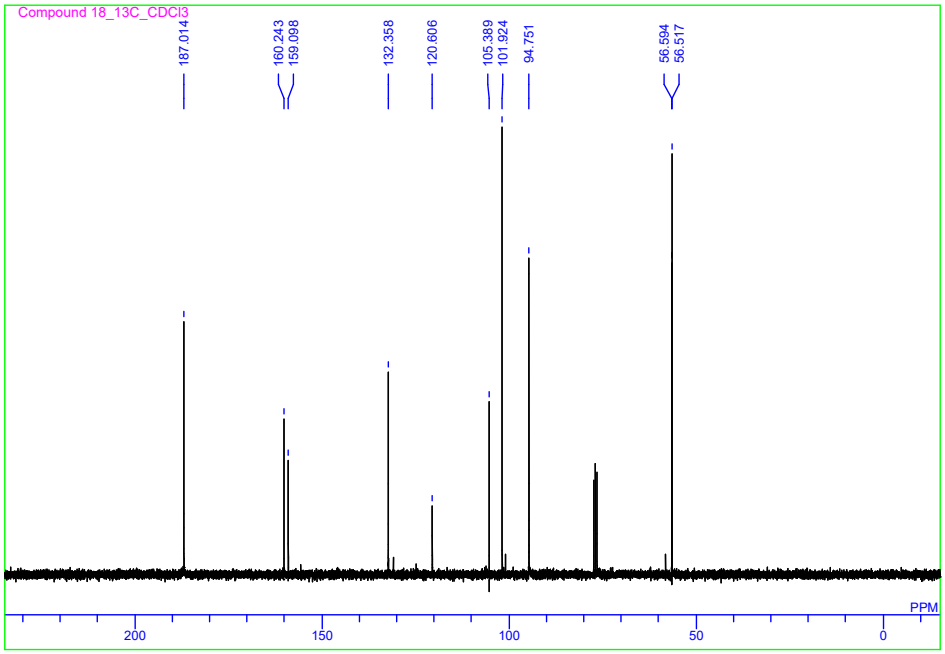

19: ^{1}H NMR chart ($CDCl_3$)

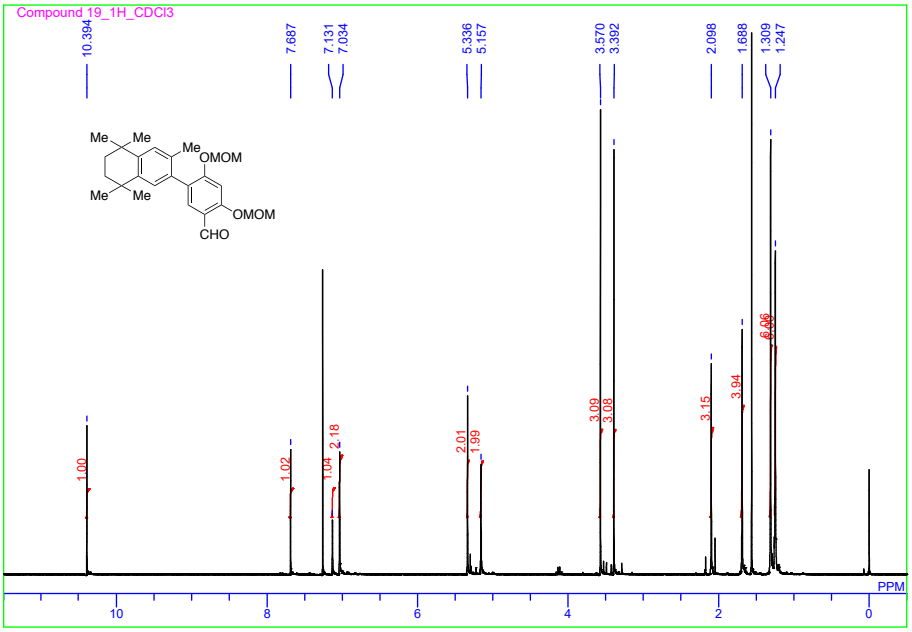

19: ^{13}C NMR chart ($CDCl_3$)

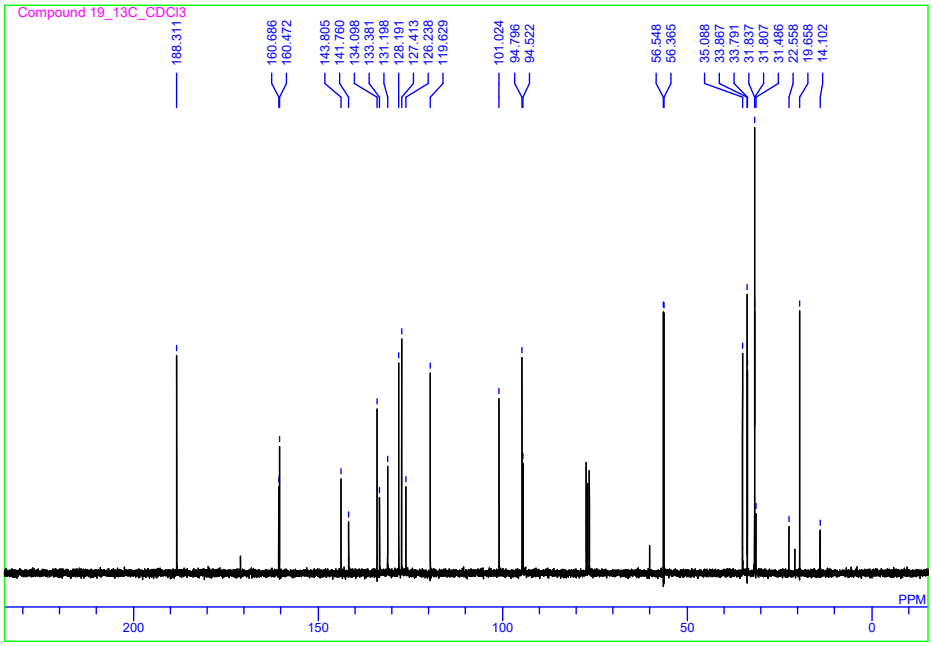

20: ^{1}H NMR chart ($CDCl_3$)

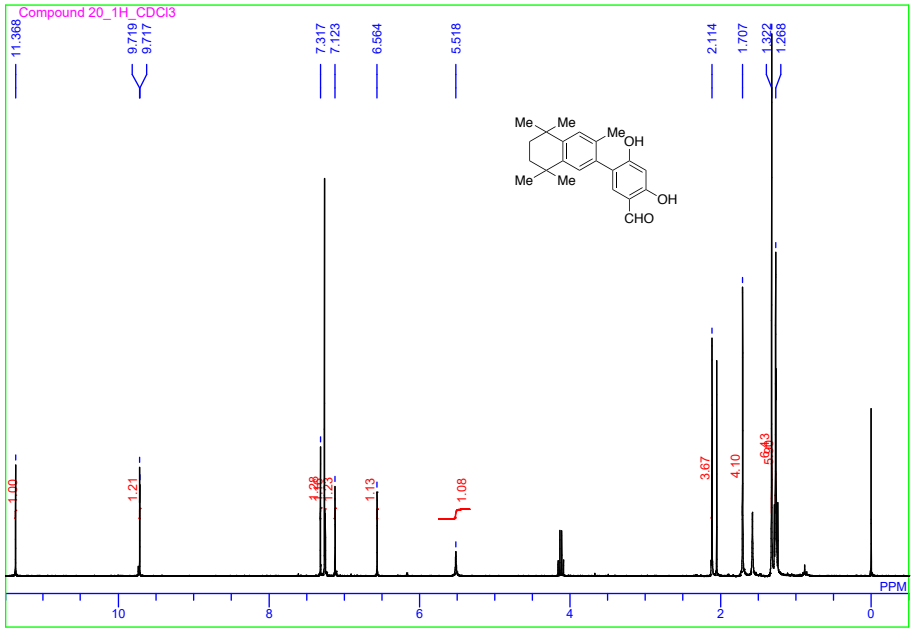

20: ^{13}C NMR chart ($CDCl_3$)

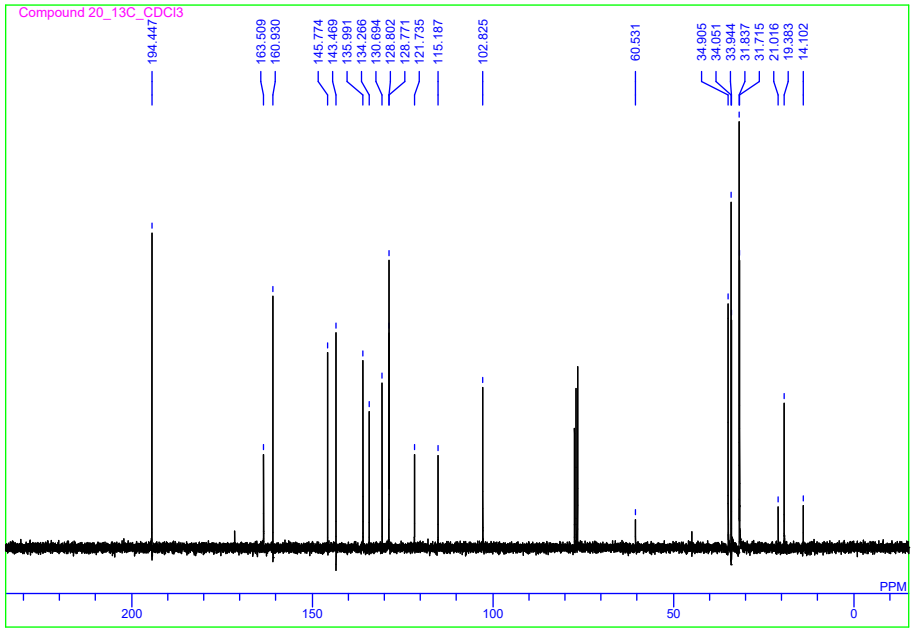

22: ^{1}H NMR chart ($CDCl_3$)

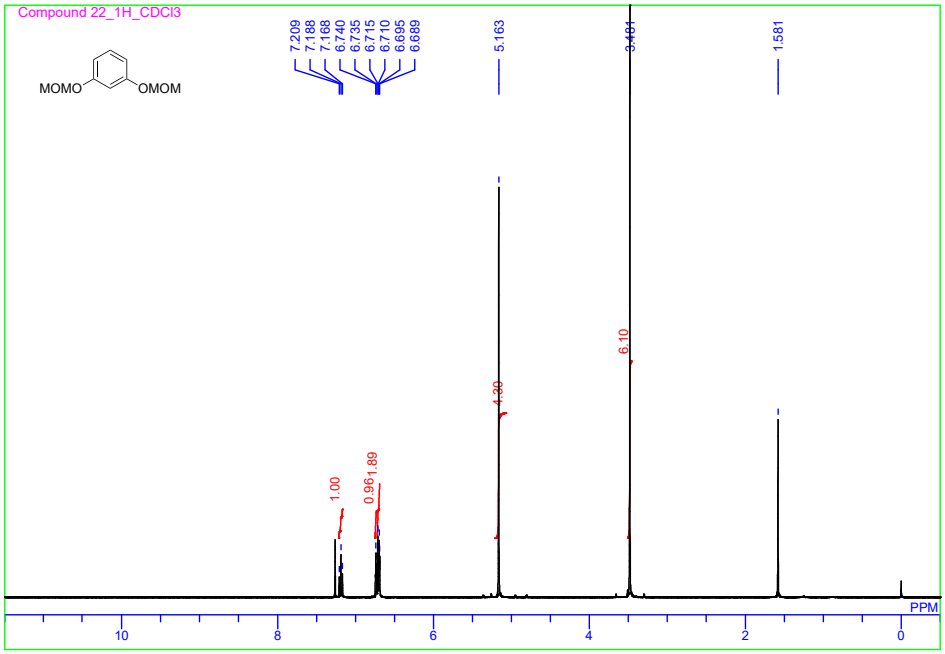

22: ^{13}C NMR chart ($CDCl_3$)

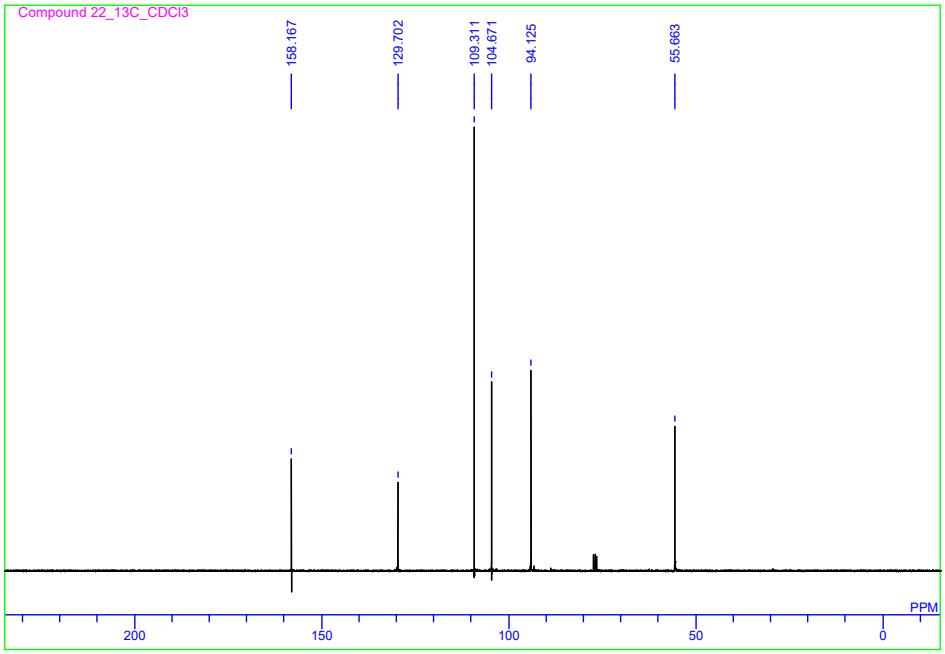

23: ^{1}H NMR chart ($CDCl_3$)

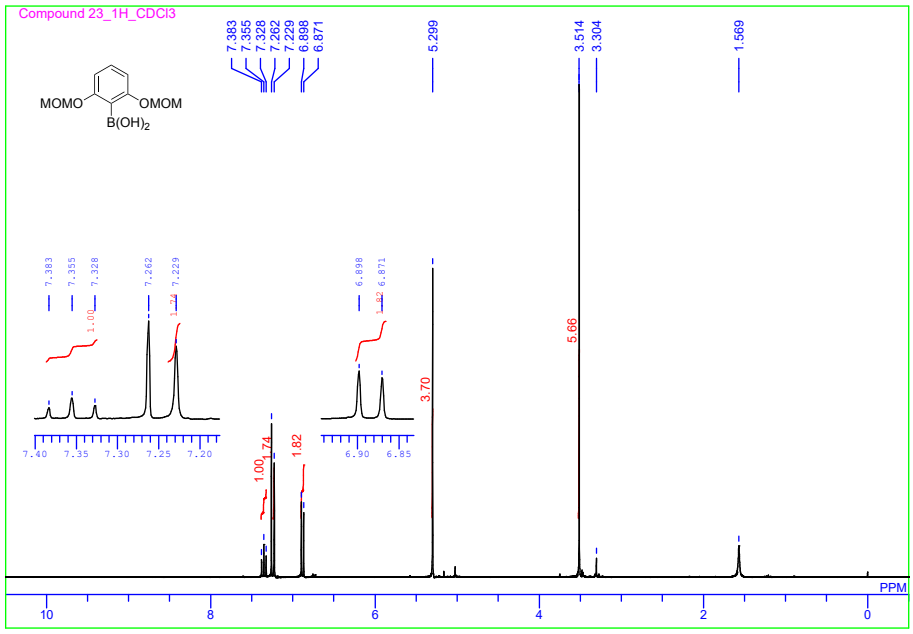

23: ^{13}C NMR chart ($CDCl_3$)

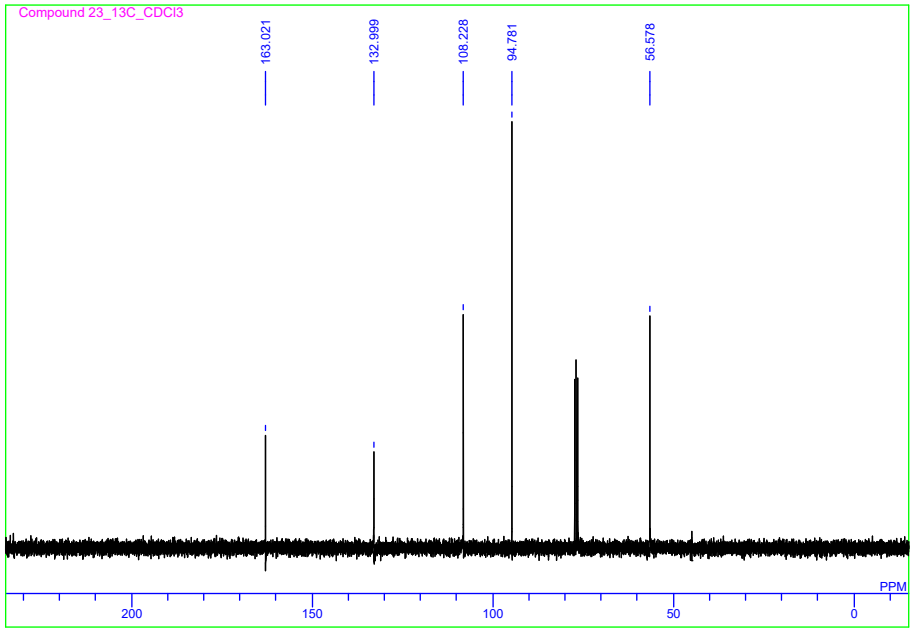

24: ^{1}H NMR chart ($CDCl_3$)

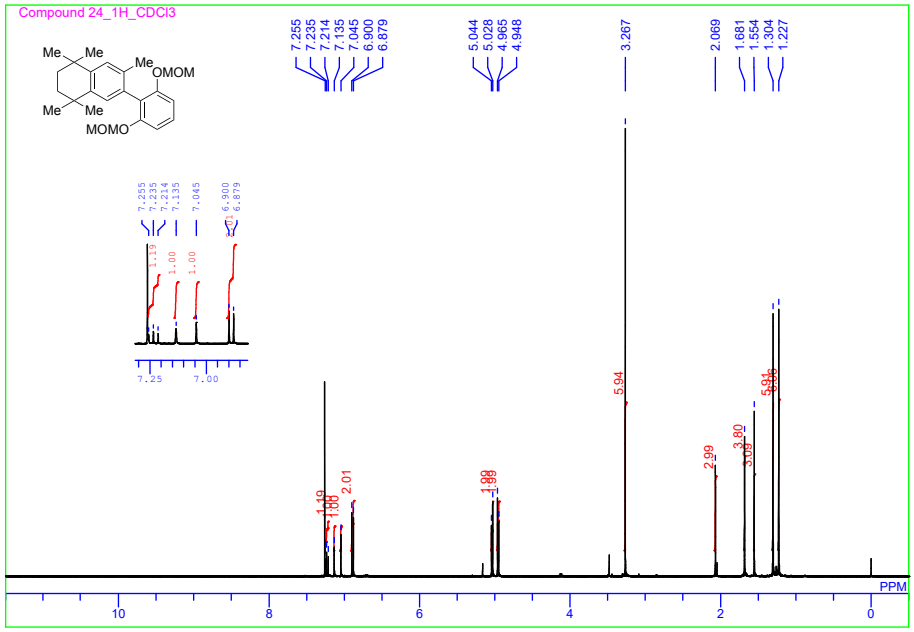

24: ^{13}C NMR chart ($CDCl_3$)

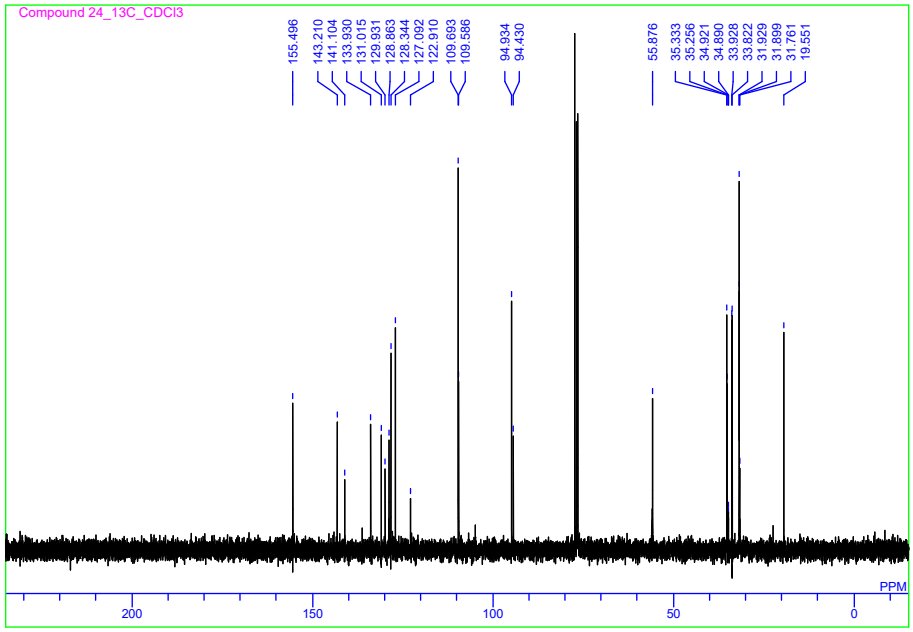

25: ^{1}H NMR chart ($CDCl_3$)

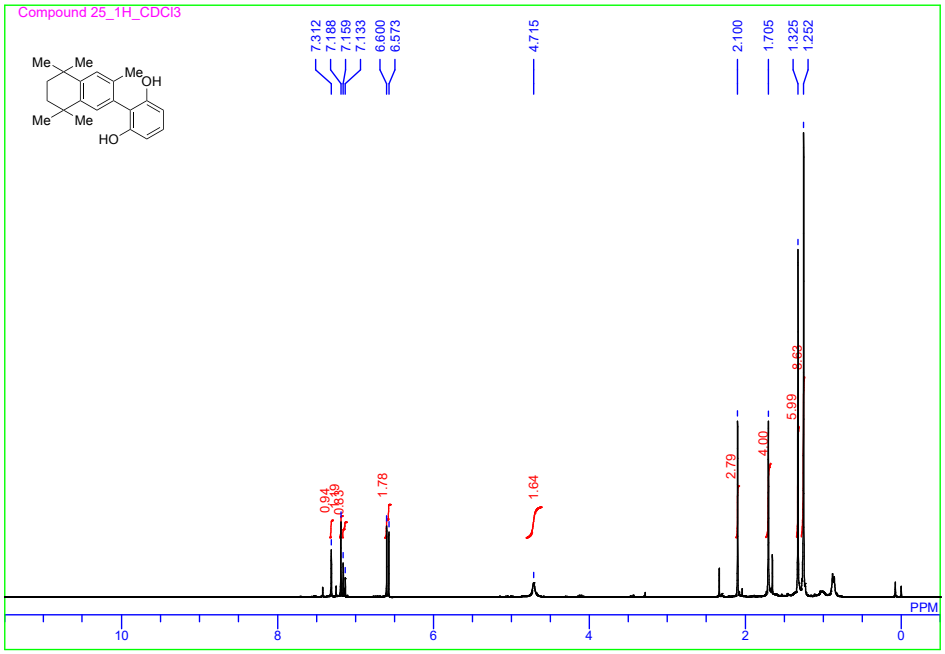

25: ^{13}C NMR chart ($CDCl_3$)

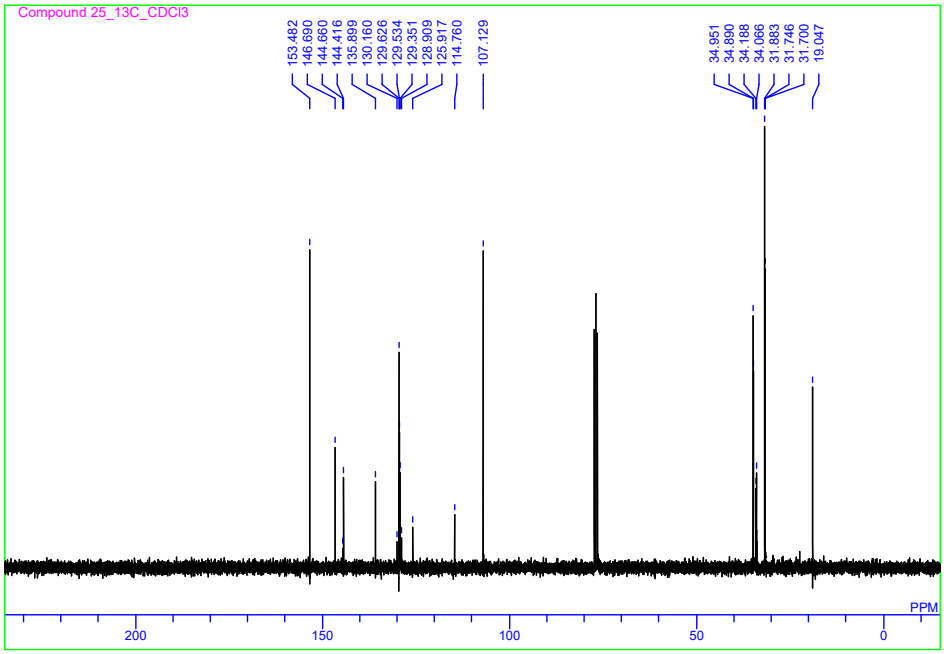

26: ^{1}H NMR chart ($CDCl_3$)

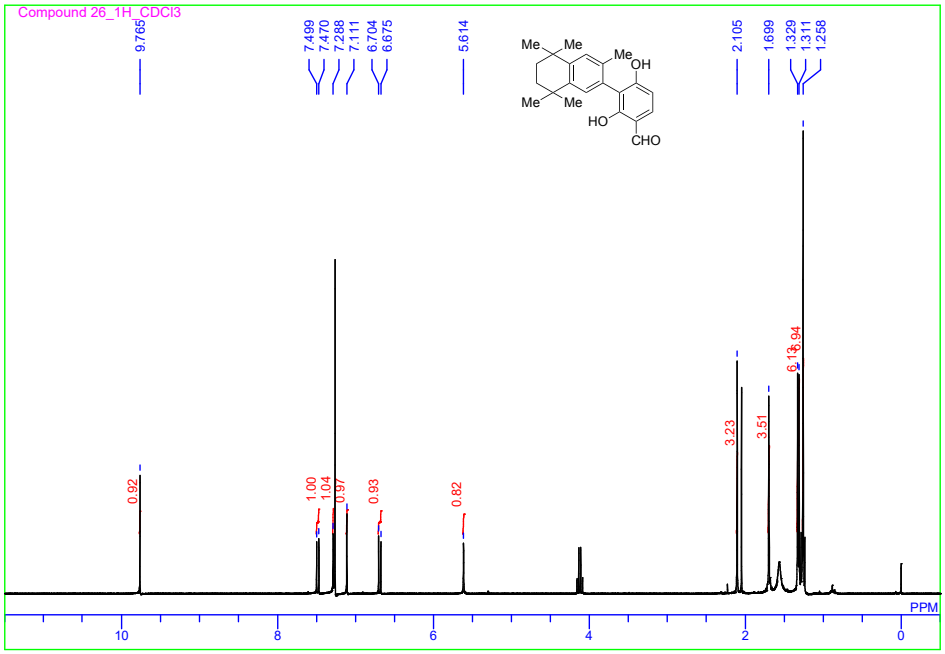

26: ^{13}C NMR chart ($CDCl_3$)

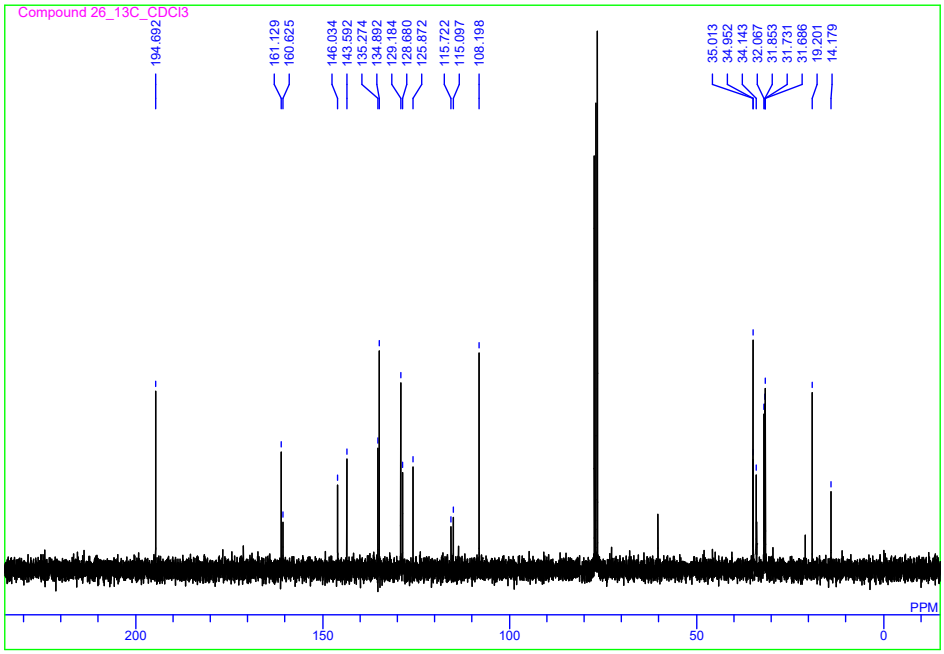

15. HPLC Charts

Compound **10**

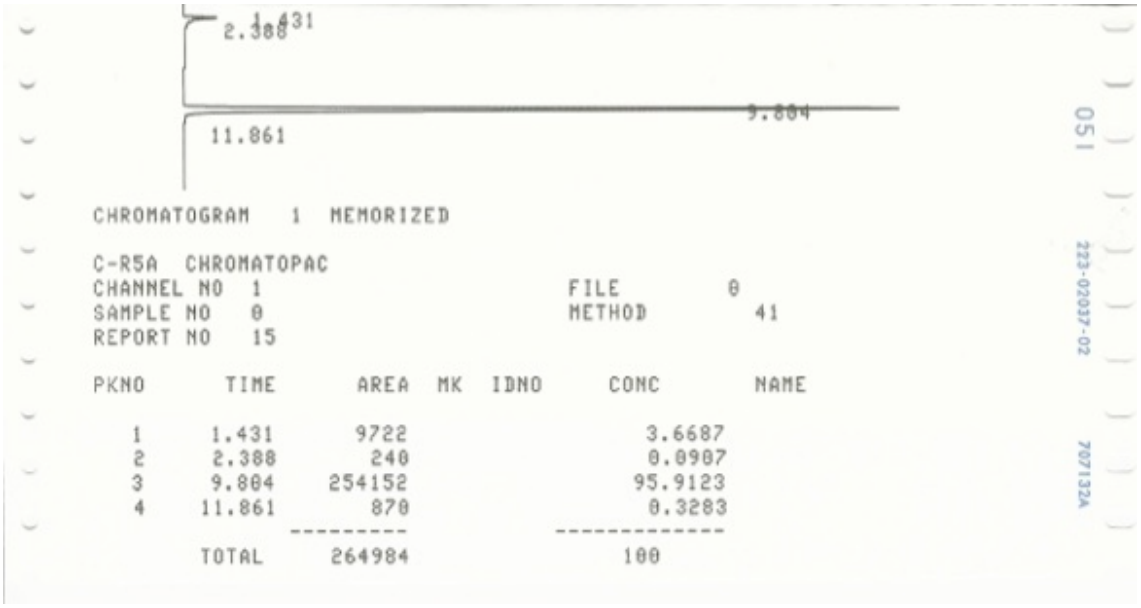

Compound **11**

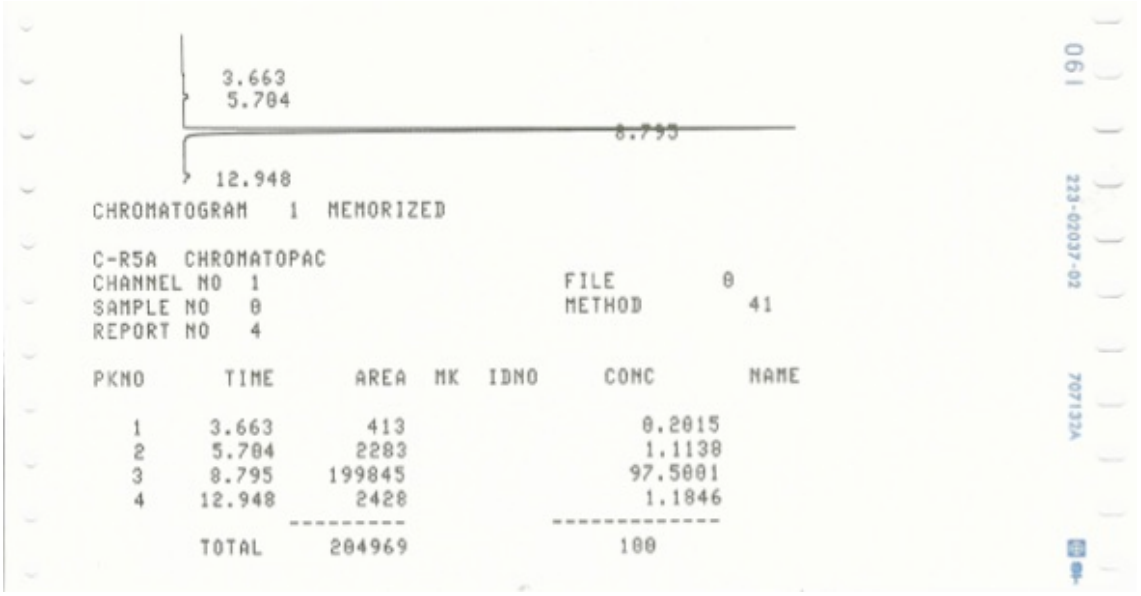

16. Acknowledgement

We thank Dr. Hiroyuki Kagechika (School of Biomedical Science, Tokyo Medical and Dental University, Tokyo, Japan) for providing PA452 and HX531.

17. References

(S1) Otwinowski, Z.; Minor, W. Processing of X-ray diffraction data collected in oscillation mode, *Methods Enzymol.*, **1997**, *276*, 307–326.

(S2) Vagin, A.; Teplyakov, A. MOLREP: an automated program for molecular replacement, *J. Appl. Crystallogr.*, **1997**, *30*, 1022–1025.

(S3) Emsley, P.; Lohkamp, B.; Scott, W.G.; Cowtan, K. Features and development of Coot. *Acta Crystallogr. D Biol. Crystallogr.*, **2010**, *66*, 486–501.

(S4) Murshudov, G.N.; Skubak, P.; Lebedev, A.A.; Pannu, N.S.; Steiner, R.A.; Nicholls, R.A.; Winn, M.D.; Long, F.; Vagin, A.A. REFMAC5 for the refinement of macromolecular crystal structures. *Acta Crystallogr. D Biol. Crystallogr.*, **2011**, *67*, 355–367.

(S5) Delano, W.L. The PyMOL molecular graphics system, (Delano Scientific, S. C., CA., Ed.) **2002**.

(S6) Fery-Forgues, S.; Lavabre, D. Are fluorescence quantum yields so tricky to measure? A demonstration using familiar stationery products. *J. Chem. Educ.*, **1999**, *76*, 1260–1264.

(S7) Fletcher, A.N. Relative fluorescence quantum yields of quinine sulfate and 2-aminopurine. *J. Mol. Spectrosc.* **1967**, *23*, 221–224.

(S8) Miyashita, Y.; Numoto, N.; Arulmozhiraja, S.; Nakano, S.; Matsuo, N.; Shimizu, K.; Shibahara, O.; Fujihara, M.; Kakuta, H.; Ito, S.; Ikura, T.; Ito, N.; Tokiwa, H. Dual conformation of

the ligand induces the partial agonistic activity of retinoid X receptor alpha (RXRalpha). *FEBS Lett.*, **2018**, *593*, 242–250.

(S9) Schultz, J. R.; Tu, H.; Luk, A.; Repa, J.J.; Medina, J.C.; Li, L.; Schwendner, S.; Wang, S.; Thoolen, M.; Mangelsdorf, D.J.; Lustig, K. D.; Shan, B. Role of LXRs in control of lipogenesis. *Genes Dev.* **2000**, *14*, 2831–2838.

(S10) Dean, R.B.; Dixon, W.J. Simplified statistics for small numbers of observations. *Anal. Chem.*, **1951**, *23*, 636–638.

(S11) Ohno, K.; Fukushima, T.; Santa, T.; Waizumi, N.; Tokuyama, H.; Maeda, M.; Imai, K. Estrogen receptor binding assay method for endocrine disruptors using fluorescence polarization. *Anal. Chem.* **2002**, *74*, 4391–4396.

(S12) Zhang, J.H.; Chung, T.D.; Oldenburg, K.R. A simple statistical parameter for use in evaluation and validation of high throughput screening assays, *J. Biomol. Screen.* **1999**, *4*, 67–73.

(S13) Takahashi, B.; Ohta, K.; Kawachi, E.; Fukasawa, H.; Hashimoto, Y.; Kagechika, H. Novel retinoid X receptor antagonists: specific inhibition of retinoid synergism in RXR-RAR heterodimer actions. *J. Med. Chem.* **2002**, 45, 3327–3330.

(S14) Ebisawa, M.; Umemiya, H.; Ohta, K.; Fukasawa, H.; Kawachi, E.; Christoffel, G.; Gronemeyer, H.; Tsuji, M.; Hashimoto, Y.; Shudo, K.; Kagechika, H. Retinoid X receptor-antagonistic diazepinylbenzoic acids. *Chem. Pharm. Bull.* **1999**, *47*, 1778–1786.

(S15) Zhang, H.; Zhou, R.; Li, L.; Chen, J.; Chen, L.; Li, C.; Ding, H.; Yu, L.; Hu, L.; Jiang, H.; Shen, X. Danthron functions as a retinoic X receptor antagonist by stabilizing tetramers of the receptor. *J. Biol. Chem.* **2011**, *286*, 1868–1875.